Published in final edited form as:
JACC Cardiovasc Imaging. 2011 November ; 4(11): 1195–1205. doi:10.1016/j.jcmg.2011.07.008.

Prevalence and Risk Factors of Carotid Vessel Wall Inflammation in Coronary Artery Disease Patients:

FDG-PET and CT Imaging Study

Jan Bucerius, MD[*,†,‡], **Raphaël Duivenvoorden, MD**[*,†,§], **Venkatesh Mani, PHD**[*,†,‖], **Colin Moncrieff**[*,†], **James H. F. Rudd, MD, PHD**[¶], **Claudia Calcagno, MD, PHD**[*,†], **Josef Machac, MD**[#], **Valentin Fuster, MD, PHD**[**,‖], **Michael E. Farkouh, MD, MSC**[††], and **Zahi A. Fayad, PHD**[*,†,‖]

[*]Translational and Molecular Imaging Institute, Mount Sinai School of Medicine, New York, New York [†]Department of Radiology, Mount Sinai School of Medicine, New York, New York [‡]Department of Nuclear Medicine, University of Bonn, Bonn, Germany [§]Department of Vascular Medicine, Academic Medical Center, Amsterdam, the Netherlands [‖]Department of Cardiology, Zena and Michael A. Weiner Cardiovascular Institute and Marie-Josée and Henry R. Kravis Cardiovascular Health Center, Mount Sinai School of Medicine, New York, New York [¶]Division of Cardiovascular Medicine, University of Cambridge, Cambridge, United Kingdom [#]Division of Nuclear Medicine, Department of Radiology, Mount Sinai School of Medicine, New York, New York [**]The Centro Nacional de Investigaciones Cardiovasculares (CNIC), Madrid, Spain [††]Cardiovascular Imaging Clinical Trials Unit, Mount Sinai School of Medicine, New York, New York

Abstract

OBJECTIVES—We investigated the prevalence and clinical risk factors of carotid vessel wall inflammation by means of ^{18}F-fluorodeoxyglucose positron emission tomography (FDG-PET) in a population consisting of coronary artery disease (CAD) patients.

BACKGROUND—The atherosclerotic disease process is characterized by infiltration and retention of oxidized lipids in the artery wall, triggering a disproportionate inflammatory response. Efforts have been made to use noninvasive imaging to quantify this inflammatory response in the vessel wall. Recently, carotid FDG-PET has been shown to reflect the metabolic rate of glucose, a process known to be enhanced in inflamed tissue.

METHODS—Carotid inflammation was quantified in 82 CAD patients (age 62 ± 10 years) as the maximum target-to-background ratio ($_{\text{wholevessel}}\text{TBR}_{\text{max}}$). Furthermore, we assessed the maximal standardized uptake value values ($_{\text{wholevessel}}\text{SUV}_{\text{max}}$), the single hottest segment (SHS), and the percent active segments (PAS) of the FDG uptake in the artery wall, measured by FDG-PET.

Reprint requests and correspondence: Dr. Zahi A. Fayad, Translational and Molecular Imaging Institute, Mount, Sinai School of Medicine, One Gustave L. Levy Place, P.O. Box 1234, New York, New York 10029. zahi.fayad@mssm.edu.

All other authors have reported that they have no relationships relevant to the contents of this paper to disclose.

RESULTS—Whole-vessel TBR_{max} > 1.8 was present in 67%, > 2.0 in 39%, > 2.2 in 23%, and > 2.4 in 12% of the population. Multiple linear regression analysis with backward elimination revealed that body mass index (BMI) ≥ 30 kg/m^2 ($p < 0.0001$), age > 65 years ($p = 0.01$), smoking ($p = 0.02$), and hypertension ($p = 0.01$) were associated with $_{wholevessel}TBR_{max}$. The number of components of the metabolic syndrome was also associated with $_{wholevessel}TBR_{max}$ ($p = 0.02$). In similar analyses, $_{wholevessel}SUV_{max}$ was associated with BMI ≥30 kg/m^2 ($p < 0.0001$), age > 65 years ($p = 0.004$), male gender ($p = 0.02$), and hypertension ($p = 0.04$); SHS with BMI ≥30 kg/m^2 ($p < 0.0001$), age >65 years ($p = 0.02$), smoking ($p = 0.04$), and hypertension ($p = 0.05$); PAS with BMI ≥30 kg/m^2 ($p = 0.001$), smoking ($p = 0.03$), and hypertension ($p = 0.01$).

CONCLUSIONS—Carotid inflammation as revealed by FDG-PET is highly prevalent in the CAD population and is associated with obesity, age over 65 years, history of hypertension, smoking, and male gender. Artery wall FDG uptake increased when components of the metabolic syndrome clustered.

Keywords

atherosclerosis; FDG-PET; inflammation; metabolic syndrome; obesity

---

The atherosclerotic disease process is characterized by infiltration and retention of oxidized lipids in the artery wall, triggering a disproportionate inflammatory response (1). Preventive strategies have focused on controlling risk factors, such as smoking, blood pressure, and serum lipid levels, which have had partial success in reducing the incidence of atherothrombotic events (2). Nonetheless, substantial residual risk remains, even when treatment goals are fully met (3).

Increasing interest has now turned to the inflammatory component of atherogenesis. Serum biomarkers of inflammation have emerged as independent predictors of coronary artery disease (CAD). In fact, a recent study in 1,117 stable CAD patients showed that subjects with both C-reactive protein (CRP) and myeloperoxidase in the highest tertile had a 5.3-fold increased risk of cardiovascular mortality compared with patients in the lowest tertiles (4). Moreover, the JUPITER (Justification for the Use of Statins in Primary Prevention: An Intervention Trial Evaluating Rosuvastatin) trial showed that identifying patients at risk by using CRP and treating them accordingly with statins can reduce cardiovascular event rates by 57% compared with placebo (5). Currently, novel pharmacotherapies that target anti-inflammatory pathways in atherosclerosis are being investigated (6).

In line with this development, efforts have been made to use noninvasive imaging to quantify vessel wall inflammation. Recently, carotid ^{18}F-fluorodeoxyglucose positron emission tomography (FDG-PET) has been shown to reflect the metabolic rate of glucose, a process known to be enhanced in inflamed tissue. In fact, FDG uptake is significantly associated with both the degree of macrophage infiltration and the levels of inflammatory gene expression in plaques (7–9). Furthermore, this noninvasive technique is capable of assessing efficacy of anti-inflammatory interventions in humans (10,11).

To further validate whether carotid FDG-PET is a surrogate marker for vessel wall inflammation, it is important to investigate the relation between FDG-PET and CAD risk

factors. A previous study showed that carotid inflammation was associated with several CAD risk factors (12). However, this retrospective study was limited by the fact that it only included cancer patients with a low prevalence of CAD. In a more recent study by Rudd et al. (13), involving 41 patients with vascular disease or multiple cardiovascular risk factors, there was significantly higher carotid FDG uptake in patients with documented CAD and in males (compared with females). A limitation of that study was the heterogeneity of the study population with respect to their cardiovascular disease burden as well as the small number of patients. Therefore, the prevalence of vessel wall inflammation and its relationship with CAD risk factors in a predefined CAD population is still not fully understood.

The aim of the current study was to assess the prevalence of carotid vessel wall inflammation as assessed by FDG-PET and to identify which clinical risk factors are associated with carotid inflammation in a population consisting of patients with documented CAD.

METHODS

Study design

This was a cross-sectional study, investigating the prevalence of carotid vessel wall inflammation and the relation between clinical risk factors and carotid inflammation as assessed by FDG-PET. The study was conducted at the Mount Sinai School of Medicine, New York. The study protocol was reviewed and approved by the institutional review board, and all subjects gave written informed consent. Inclusion criteria were males and females with a diagnosis of CAD. CAD was defined as a history of myocardial infarction, percutaneous transluminal coronary intervention or coronary artery bypass surgery. Subjects with previous carotid surgery or fasting glucose levels ≥11.1 mmol/l were excluded (14).

Questionnaire, and biometric and biochemical measurements

Presence of cardiovascular risk factors, use of medication, and family history of CAD were assessed by a questionnaire. Presence of hypertension was defined as a history systolic blood pressure > 140 mm Hg, or a diastolic blood pressure > 90 mm Hg. Diabetes was defined as use of an antidiabetic treatment (diet, oral, parenteral). Weight and height were measured to calculate body mass index (BMI). Fasting glucose levels were obtained by fingerstick blood glucose measurements (Accu-Chek Advantage, Roche Diagnostics, Indianapolis, Indiana) prior to FDG administration.

FDG-PET/computed tomography imaging

FDG-PET/computed tomography (CT) was performed after an overnight fast using a GE Healthcare (Milwaukee, Wisconsin) LightSpeed Discovery ST PET/CT scanner (14, 15). FDG was administered intravenously (562.4 ± 81.4 MBq), and patients rested comfortably for 99 to 193 min before the scan of the neck was started. A low-dose CT scan (140 kV, 80 mA, and 4.25-mm slice thickness) was performed for attenuation correction and co-registration. No CT contrast agent was administered. Head and neck were placed into a head holder for imaging of the carotids. Images from 1 bed position (15.5 cm) with coverage

extending inferior to the internal auditory meatus were acquired in 3-dimensional mode for 15 min.

Image analysis

Image analysis was performed on a dedicated, commercially available workstation (Extended Brilliance Workspace V4.0.0.3206, Philips Medical Systems Inc., Cleveland, Ohio). An experienced reader (J.B.) analyzed all scans. To assess intraobserver agreement, a subset of 15 randomly assigned scans were analyzed twice by the same reader, with a minimum of 14 days between the first and second reading to avoid recall bias.

After loading the PET and CT images, the general imaging quality was reviewed, and as applicable, the following parameters were also reviewed: optimal counts, coverage, and image reconstruction of both carotids, and co-registration of the PET and CT images. Data were excluded from the analysis if significant motion artifact, as assessed by blurring edges of the CT and/or movement between the PET and CT co-registered images was present. In general, each slice of the fused PET/CT was judged as 1 segment of the carotids. The carotid artery was divided anatomically into common, internal, and external carotid arteries, respectively. Only the common carotid artery up to the bifurcation was analyzed on both sides of the neck in order to ensure a correct identification of the vessel anatomy and to minimize the impact of FDG uptake in surrounding structures. Slices where the anatomy of the artery could not be identified with certainty or those slices with a high FDG uptake in the surrounding tissue/structures (affecting the FDG uptake within the vessel) were excluded from further analysis. Arterial FDG uptake was quantified by drawing a region of interest (ROI) around each artery on every slice of the co-registered transaxial PET/CT images (Fig. 1). Next, the maximal arterial standardized uptake value (SUV_{max}) was calculated as the maximal pixel activity within the ROI of every slice of the vessel. The SUV is the decay-corrected tissue concentration of FDG in kilobecquerels per milliliter, adjusted for the injected FDG dose and the body weight of the patient, and is a well-recognized method for quantification of FDG-PET data (16). By averaging the maximum SUV values of all arterial slices of the left and right carotid arteries, a $_{wholevessel}SUV_{max}$ value was derived for the carotid arteries. The maximal arterial target-to-background ratio (TBR_{max}) was then calculated by correcting the SUV_{max} for blood activity. This was done by dividing the SUV_{max} values in the artery by the average blood SUV_{mean}estimated from both jugular veins to produce a blood-corrected artery SUV. This is considered to be a reflection of arterial FDG uptake (17). For evaluation of the mean FDG blood pool uptake, as depicted by the mean SUV_{mean}, at least six 3- to 4-mm ROIs were placed in consecutive slices of both jugular veins and averaged. Corrected SUV_{max} values were than averaged in order to derive a $_{wholevessel}TBR_{max}$ for both carotid arteries. Additionally, we identified the single hottest segment (SHS), defined as the highest TBR_{max} value of the carotid arteries, as well as the percent active segments (PAS) of each common carotid artery. PAS reflects the percentage of all segments of ether the left or right carotid artery above a pre-defined threshold, namely $TBR_{max} > 1.9$. This threshold was determined by calculating the median of all $_{wholevessel}TBR_{max}$ values ($TBR_{max} > 1.9$) of the included patients.

In order to provide information about the prevalence of different degrees of FDG uptake in both common carotid arteries, we defined 4 different potential cutoff values for vessel wall inflammation, namely $_{wholevessel}TBR_{max}$ > 1.8, > 2.0, > 2.2, and > 2.4 based on the results of a previously published study by Tawakol et al. (7).

Statistical analysis

All continuous variables are expressed as mean ± SD, and categorical data as absolute numbers and percentages throughout this paper.

Multiple linear regression analysis with backward elimination was used to assess the association between CAD risk factors and $_{wholevessel}TBR_{max}$, $_{wholevessel}SUV_{max}$SHS, and PAS. Whole-vessel TBR_{max}, $_{wholevessel}SUV_{max}$, SHS, and PAS were the response variables, and CAD risk factors the explanatory variables. The explanatory variables included were age > 65 years, male gender, BMI ≥30 kg/m^2, smoking, hypertension, alcohol use, exercising, diabetes, fasting glucose levels, and family history of cardiovascular disease. Variables were retained if $p < 0.10$. Multiple linear regression analyses were also performed to assess the association between each of these retained individual CAD risk factors and $_{wholevessel}TBR_{max}$, $_{wholevessel}$-SUV_{max}, and SHS, as well as PAS. The $_{wholevessel}TBR_{max}$, $_{wholevessel}SUV_{max}$, SHS, and PAS were taken as the response variables, and each of the aforementioned CAD risk factors as the explanatory variable, adjusting for the other risk factors (BMI ≥30 kg/m^2, age > 65 years, hypertension, smoking, male gender) as potential confounders. To assess the relation between the number of components of the metabolic syndrome and $_{wholevessel}TBR_{max}$, a 1-way analysis of variance was performed to test for between-group differences. To assess the intraobserver agreement of the image analysis, intraclass correlation coefficients with 95% confidence intervals were calculated in a subgroup of patients who underwent vascular FDG-PET imaging at our institution (18). Depending on normal distribution, the Pearson or Spearman rho correlation coefficients (r) were calculated to assess the relation between FDG circulation time (i.e., the time interval between FDG injection and starting time of the carotid data acquisition), acquired counts in the carotids, injected FDG dose, and $_{wholevessel}TBR_{max}$, as well as between the different FDG uptake parameters. All statistical analyses were performed using SPSS statistical package 16.0 (SPSS Inc., Chicago, Illinois).

RESULTS

Population characteristics

A total of 82 patients were included in the study, of which all underwent FDG-PET/CT imaging. In 3 of the 82 patients, FDG-PET analysis could not be performed due to high FDG uptake in the thyroid, affecting the visualization and analysis of FDG uptake within the carotid arteries, leaving 79 eligible patients for image analysis. Patient characteristics are shown in Table 1.

FDG-PET imaging and CAD risk factors

Values for $_{wholevessel}TBR_{max}$, $_{wholevessel}SUV_{max}$, SHS, and PAS, as well as prevalence of different cutoff values for $_{wholevessel}TBR_{max}$, are shown in Table 1. Comparison of the 4

different FDG uptake parameters showed highly significant positive correlations between all FDG uptake values ($r > 0.64$; $p < 0.0001$ for all comparisons).

Multivariate linear regression analysis with backward elimination, showing the relation between CAD risk factors and the various FDG-PET parameters, are shown in Table 2. BMI ≥30 kg/m^2, age > 65 years, hypertension, smoking, and male gender are shown to be strong determinants of the FDG uptake in the carotid artery walls.

Furthermore, multivariate linear regression analysis showed that BMI ≥30 kg/m^{2}age > 65 years, hypertension, and smoking were independent risk factors for carotid inflammation as depicted by $_{wholevessel}TBR_{max}$ (Fig. 2). Further analysis revealed that the number of components of the metabolic syndrome was significantly associated with $_{wholevessel}TBR_{max}$ (Fig. 3). Independent predictors for $_{wholevessel}SUV_{max}$, SHS, and PAS values are shown in Figure 4.

FDG-PET methodology

Concerning the intraobserver variability, intraclass correlation coefficient values for $_{wholevessel}TBR_{max}$ were 0.98 (0.94 to 0.99) for the left and 0.97 (0.90 to 0.99) for the right carotid, indicating excellent agreement. The mean time difference between first and second reading was 29.1 days, with a range of 14 to 55 days.

No correlation was observed between $_{wholevessel}TBR_{max}$ and FDG circulation time ($r = 0.20$, $p = 0.08$), acquired counts in the carotids ($r = -0.07$, $p = 0.57$), or injected FDG dose ($r = 0.15$, $p = 0.18$).

DISCUSSION

The aim of our study was to determine the prevalence of carotid vessel wall inflammation, quantified by FDG-PET, in a CAD population and to identify which cardiovascular risk factors are related to carotid inflammation. We demonstrate that low-grade vessel wall inflammation is frequent in the CAD population. In addition, we show that BMI ≥30 kg/m^{2}age > 65 years, history of hypertension, smoking, and male gender are important clinical risk factors for carotid FDG uptake. Moreover, FDG uptake in the vessel wall showed a high correlation with the number of components of the metabolic syndrome. These findings may be important since histology studies have shown that plaque inflammation is associated with plaque rupture and atherothrombotic events (19). Our results imply that vessel wall inflammation may persist despite medical therapy, even at the highest $_{wholevessel}TBR_{max}$ cutoff value.

Whether vessel wall inflammation measured by FDG-PET is related to the occurrence of future cardiovascular events is currently being investigated in large longitudinal follow-up studies (20). The determination of the prevalence of low-grade carotid inflammation depends on the choice of the cutoff TBR_{max} value. It remains a matter of debate as to whether the vessel wall is considered “inflamed.” Histological studies of plaques obtained after carotid endarterectomy have shown that symptomatic plaques have higher macrophage content than asymptomatic plaques (21–23). Jander et al. (22) revealed that the percentage

of macrophage-rich area of the plaque was 18 ± 10% in recently symptomatic patients versus 11 ± 4% in asymptomatic patients with carotid stenosis (p = 0.005). Obviously, there is some overlap between these groups, so pinpointing an exact number of macrophages to determine inflammation is difficult. However, it does provide an order of magnitude in which macrophage content is clinically relevant. To translate this into meaningful FDG-PET–related cutoff values poses another challenge. Tawakol et al. (7) performed in vivo FDG-PET imaging in 17 patients that subsequently underwent carotid endarterectomy. These authors showed that plaque macrophage content was related to a gradual increase in plaque FDG uptake. Most plaques with TBR values under 1.8 had macrophage areas in the range of 0% to 5%, lesions with TBRs between 1.8 and 2.8 had 5% to 15% macrophages, and plaques with TBRs above 2.8 had macrophage areas > 15% (7). For our study, in order to provide an estimate about the different degrees of FDG uptake in our study population, we felt it reasonable to set TBR cut points between 1.8 and 2.4 on the basis of the aforementioned pathologically derived values.

Clinical risk factors and vessel wall inflammation

We observed that obesity, aging, history of hypertension, smoking, and male gender were independent predictors of carotid inflammation as depicted by FDG-PET. By far the strongest determinant for all different FDG uptake parameters was increased BMI. Furthermore, we found a significant relation between the metabolic syndrome and vessel wall inflammation. Our findings are in line with previous publications. In a retrospective study in patients that underwent FDG-PET imaging for cancer screening, Tahara et al. (12) showed that carotid inflammation was associated with waist circumference, hypertension, glucose intolerance, and the metabolic syndrome. The similarities with our findings are striking, considering the fact that very different populations were investigated. We investigated a CAD population, whereas only 12.5% of their population had a history of CAD. Moreover, compared with our study, the number of men (68% vs. 82%), BMI (24 ± 3 kg/m^2 vs. 28 ± 4 kg/m^2), history of hypertension (42% vs. 72%), and the number of diabetic patients (7% vs. 38%) were all markedly lower. Furthermore, in contrast to the current report, their study was performed on a standalone PET scanner only, and they did not apply a vascular-tailored imaging protocol. Despite these differences, both studies revealed that obesity and the number of components of the metabolic syndrome were strong determinants of carotid inflammation (12). In a more recent prospective trial in patients with known CAD or multiple cardiovascular risk factors, Rudd et al. (13) found carotid FDG uptake to be significantly higher in patients with known CAD and in males versus females. Their results are in broad agreement, not only with the study by Tahara et al. (12) mentioned in the previous text, but also with the results of our study, all indicating higher FDG uptake in the carotids of men compared with women (12, 13). This observation suggests that atherosclerotic plaques in men may be more highly inflamed, perhaps providing a pathological link for their higher rate of cardiovascular events. However, the number of patients in our study was twice that of the study by Rudd et al. (13), providing greater statistical power. Furthermore, similar to the study population by Tahara et al. (12), the number of men (73% vs. 82%), BMI (26 ± 5 kg/m^2 vs. 28 ± 4 kg/m^2), history of hypertension (61% vs. 72%), and the number of smokers and ex-smokers (49% vs. 55%) were again all markedly lower in their study, whereas the number of diabetic subjects were

similar to that of our study (37% vs. 38%). Additionally, as with the study by Tahara et al. (12), the study population by Rudd et al. (13) was more heterogeneous compared with that in the current trial, which only includes patients with documented CAD.

The results of the present study have important clinical implications. Patients with the aforementioned characteristics might benefit most from anti-inflammatory pharmacotherapy. A currently widely available therapy known to exhibit anti-inflammatory properties in addition to serum lipid lowering is 3-hydroxy-3-methyl-glutaryl-CoA reductase (statins) (5). Novel anti-inflammatory drugs being investigated as potential antiatherosclerotic therapies are compounds such as inhibitors of lipoprotein-associated phospholipase A2, anti-integrin and anticytokine therapies, and mycophenolate mofetil, as well as vaccination with lipoprotein peptides (6, 24). Furthermore, high-density lipoprotein cholesterol (HDL) is known to have anti-inflammatory properties, and drugs that increase HDL by cholesteryl ester transfer protein inhibition are currently being investigated in phase II and phase III trials (25, 26).

To assess the efficacy and safety of these novel compounds, longitudinal follow-up studies assessing clinical endpoints will need to be performed. However, such studies are expensive and time consuming, and expose many patients to a drug of which the benefit or potential harm is unknown. Therefore, prior to embarking on such studies, efficacy can be investigated by use of surrogate imaging markers (27). Imaging FDG uptake by the vessel wall has emerged as a valuable surrogate marker of vessel wall inflammation (28). The results of our current study suggest that assessing the efficacy of novel cardiovascular drugs with anti-inflammatory properties might best be performed in obese or metabolic syndrome patients.

The fact that obesity and the metabolic syndrome show such a strong relation with FDG uptake in the vessel wall is intriguing. The metabolic syndrome is characterized by the clustering of obesity, insulin resistance, dyslipidemia, and hypertension (29). A meta-analysis in data from 172,573 patients showed that the metabolic syndrome increases the risk for atherothrombotic events and death, with a relative risk of 1.78 (95% confidence interval: 1.58 to 2.00) (30). Chronic low-grade inflammation, as reflected by serum biomarkers, is known to accompany the occurrence of obesity and the metabolic syndrome. In fact, epidemiological studies have shown a clear relation between obesity, metabolic syndrome, and increased levels of inflammatory markers such as tumor necrosis factor α (TNF-α), interleukin 6 (IL-6), and CRP (31). A growing body of evidence supports a common pathological mechanism linking obesity to inflammation, insulin resistance, and cardiovascular disease. Adipose tissue, in addition to storing fat, is known to produce numerous cytokines and hormones (31). Studies have shown that adipocytes in obese subjects recruit macrophages, a process mediated by monocytes chemoat-tractant protein-1 (MCP-1) (31). Activation of the innate immune system occurs via toll-like receptors and receptors for advanced glycation end products that affect intracellular transcription pathways such as the nuclear factor κB (NF-κB) and the c-Jun N-terminal kinase (JNK) pathways (32). In the presence of inflammatory cells, adipocytes increase their secretion of adipokines such as adiponectin and TNF-α, which are known to directly instigate endothelial dysfunction (31). TNF-α, IL-6, and adiponectin also cause insulin resistance that induces

oxidative stress and endothelial dysfunction (32, 33). Kim et al. (34) observed a positive correlation between insulin resistance and adiponectin levels but a negative correlation between the maximum TBR levels and adiponectin. This finding is confirmed by 2 recently published studies (35, 36), which also found an inverse relationship between adiponectin and arterial inflammation as assessed by FDG uptake. Since adiponectin is known to act as a brake on inflammation, and is therefore vascular protective, in both healthy individuals and those with vascular disease, it is intriguing that in those with the highest levels of this hormone, there were the lowest degrees of FDG arterial uptake (13,34–37). In addition to the pro-atherogenic inflammatory state, obesity is also associated with hypertension and increased very low–density lipoprotein cholesterol, triglycerides, and decreased HDL cholesterol (38), which might indirectly stimulate invasion of the vessel wall by monocytes. Together, these data indicate there is a direct pathophysiological link between obesity, inflammation, and atherosclerosis. Our data support the concept that obesity and the metabolic syndrome are related to vessel wall inflammation.

Of further interest is that we found a relation between smoking and carotid inflammation. Similar to obesity, smoking has shown to induce a proinflammatory state mediated by similar mechanisms as previously discussed, with elevated levels of TNF-α, IL-6, adiponectin and CRP, insulin resistance, oxidative stress, and endothelial dysfunction (33).

FDG-PET/CT methodology-related issues

In the present study, image analyses were performed by 1 experienced reader. This might reduce statistical noise related to interobserver variation, but concerns might arise about intraobserver bias. However, the blinded and randomized intraobserver agreement measurements revealed very favorable results, indicating that image analyses by 1 reader can be sufficient for the analysis being performed.

For all trials with FDG-PET imaging, concerns may arise about the impact of methodologically related variables, such as FDG circulation time, injected FDG dose, and the acquired counts. Although minimized by the use of standardized imaging protocols, such variations inevitably occur. Therefore, we investigated whether FDG circulation time, injected FDG dose, and the acquired counts were associated with $_{\text{wholevessel}}\text{TBR}_{\text{max}}$, and observed that none of the methodologically related variables significantly impacted the FDG uptake. Therefore, it seems unlikely this could have introduced bias in our study. Furthermore, as we did not observe a clear difference in results between those patients given high FDG doses and those given low doses, our results suggest that lower FDG doses could be used in future imaging studies.

Evaluation of cardiovascular risk factors for vessel wall inflammation yielded quite consistent results for $_{\text{wholevessel}}\text{TBR}_{\text{max}}$, $_{\text{wholevessel}}\text{SUV}_{\text{max}}$, SHS, and PAS values. Because of these consistent results among the FDG uptake parameters, we do not believe that the results of the present study have been overly influenced by methodological issues related to the chosen way of image analysis. Furthermore, our work might add to the current discussion regarding the most appropriate way of assessing vessel wall inflammation, including the pros and cons of using the corrected TBR or the uncorrected SUV FDG uptake values.

Study limitations

There are some limitations of our study. First, we did not obtain serum lipid levels, markers of glucose metabolism, or serum inflammatory markers. This would have provided more complete information and more accurate determination of the metabolic syndrome. Second, this is a cross-sectional study. Therefore, we could not address whether there was a causal relationship between the presence of risk factors and vessel wall inflammation. Third, we cannot provide more detailed information about structural features of the carotid walls (calcification, lipid core) because we performed a non–contrast-enhanced CT as part of the PET/CT in order to reduce radiation exposure to patients. Furthermore, as we did not perform magnetic resonance imaging to avoid additional scanning time for the patients, morphological data from a second imaging method are also not available. Future studies, focusing on new combined imaging methods such as PET/magnetic resonance imaging, should allow this. Finally, it is unknown whether vessel wall inflammation measured by FDG-PET/CT is predictive of future cardiovascular events. Longitudinal, prospective studies testing this possibility are underway, although preliminary retrospective reports are supportive of the hypothesis (39, 40).

CONCLUSIONS

In the current study, we show that vessel wall inflammation as quantified by FDG-PET/CT is highly prevalent in the CAD population. Obesity, age over 65 years, a history of hypertension, and smoking seem to be important risk factors for carotid inflammation. Clustering of components of the metabolic syndrome also showed a strong relation with vessel wall inflammation. The results were consistent across several FDG measured endpoints that correlate with underlying inflammation. Finally, the administered activity of FDG did not affect the results, suggesting that future studies might use lower doses than previously, thereby reducing the radiation exposure to each subject.

Acknowledgments

The authors thank Ash Rafique, RT, BS, CNMT, for his assistance with the image acquisitions.

This work was partly supported by the NIHR Cambridge Biomedical Research Centre (J.H.F.R.), and by a National Institutes of Health/National Heart Lung and Blood Institute grant R01 HL071021 (Z.A.F.). Dr. Machac has received funding for scientific studies/trials from Philips Medical Systems and Lantheus Medical Imaging. H. William Strauss, MD, served as Guest Editor of this paper.

ABBREVIATIONS ANDACRONYMS

BMI	body mass index
CAD	coronary artery disease
CT	computed tomography
FDG-PET	^{18}F-fluorodeoxyglucose positron emission tomography
HDL	high-density lipoprotein cholesterol
PAS	percent active segments

ROI	region of interest
SHS	single hottest segment
SUV	standardized uptake value
TBR	target-to-background ratio

REFERENCES

1. Libby P, Ridker PM, Hansson GK. Inflammation in atherosclerosis: from pathophysiology to practice. J Am Coll Cardiol. 2009; 54:2129–2138. [PubMed: 19942084]
2. Grundy SM, Cleeman JI, Merz CN, et al. Coordinating Committee of the National Cholesterol Education Program. Implications of recent clinical trials for the National Cholesterol Education Program Adult Treatment Panel III guidelines. J Am Coll Cardiol. 2004; 44:720–732. [PubMed: 15358046]
3. Libby P. The forgotten majority: unfinished business in cardiovascular risk reduction. J Am Coll Cardiol. 2005; 46:1225–1228. [PubMed: 16198835]
4. Heslop CL, Frohlich JJ, Hill JS. Myeloperoxidase and C-reactive protein have combined utility for long-term prediction of cardiovascular mortality after coronary angiography. J Am Coll Cardiol. 2010; 55:1102–1109. [PubMed: 20223364]
5. Ridker PM, Danielson E, Fonseca FA, et al. JUPITER Study Group. Rosuvastatin to prevent vascular events in men and women with elevated C-reactive protein. N Engl J Med. 2008; 359:2195–2207. [PubMed: 18997196]
6. Libby P, Ridker PM, Hansson GK. Leducq Transatlantic Network on Atherothrombosis. Inflammation in atherosclerosis: from pathophysiology to practice. J Am Coll Cardiol. 2009; 54:2129–2138. [PubMed: 19942084]
7. Tawakol A, Migrino RQ, Bashian GG, et al. In vivo 18F-fluorodeoxyglucose positron emission tomography imaging provides a noninvasive measure of carotid plaque inflammation in patients. J Am Coll Cardiol. 2006; 48:1818–1824. [PubMed: 17084256]
8. Rudd JH, Warburton EA, Fryer TD, et al. Imaging atherosclerotic plaque inflammation with [18F]-fluorodeoxyglucose positron emission tomography. Circulation. 2002; 105:2708–2711. [PubMed: 12057982]
9. Pedersen SF, Graebe M, Fisker Hag AM, Højgaard L, Sillesen H, Kjaer A. Gene expression and 18FDG uptake in atherosclerotic carotid plaques. Nucl Med Commun. 2010; 31:423–429. [PubMed: 20145577]
10. Tahara N, Kai H, Ishibashi M, et al. Simvastatin attenuates plaque inflammation: evaluation by fluorodeoxyglucose positron emission tomography. J Am Coll Cardiol. 2006; 48:1825–1831. [PubMed: 17084257]
11. Lee SJ, On YK, Lee EJ, Choi JY, Kim BT, Lee KH. Reversal of vascular 18F-FDG uptake with plasma high-density lipoprotein elevation by atherogenic risk reduction. J Nucl Med. 2008; 49:1277–1282. [PubMed: 18632820]
12. Tahara N, Kai H, Yamagishi S, et al. Vascular inflammation evaluated by [18F]-fluorodeoxyglucose positron emission tomography is associated with the metabolic syndrome. J Am Coll Cardiol. 2007; 49:1533–1539. [PubMed: 17418291]
13. Rudd JH, Myers KS, Bansilal S, et al. Relationships among regional arterial inflammation, calcification, risk factors, and biomarkers: a prospective fluorodeoxyglucose positron-emission tomography/computed tomography imaging study. Circ Cardiovasc Imaging. 2009; 2:107–115. [PubMed: 19808576]
14. Rudd JH, Myers KS, Bansilal S, et al. (18)Fluorodeoxyglucose positron emission tomography imaging of atherosclerotic plaque inflammation is highly reproducible: implications for atherosclerosis therapy trials. J Am Coll Cardiol. 2007; 50:892–896. [PubMed: 17719477]

15. Kinahan PE, Rogers JG. Analytic 3D image reconstruction using all detected events. IEEE Trans Nucl Sci. 1989; 36:964–968.
16. Shankar LK, Hoffman JM, Bacharach S, et al. National Cancer Institute. Consensus recommendations for the use of 18F-FDG PET as an indicator of therapeutic response in patients in National Cancer Institute trials. J Nucl Med. 2006; 47:1059–1066. [PubMed: 16741317]
17. Tawakol A, Migrino RQ, Hoffmann U, et al. Noninvasive in vivo measurement of vascular inflammation with F-18 fluorodeoxyglucose positron emission tomography. J Nucl Cardiol. 2005; 12:294–301. [PubMed: 15944534]
18. Eliasziw M, Young SL, Woodbury MG, Fryday-Field K. Statistical methodology for the concurrent assessment of interrater and intrarater reliability: using goniometric measurements as an example. Phys Ther. 1994; 74:777–788. [PubMed: 8047565]
19. van der Wal AC, Becker AE, van der Loos CM, Das PK. Site of intimal rupture or erosion of thrombosed coronary atherosclerotic plaques is characterized by an inflammatory process irrespective of the dominant plaque morphology. Circulation. 1994; 89:36–44. [PubMed: 8281670]
20. The HRP Initiative. [Accessed June 3, 2011] The HRP website. Available at: http://www.hrpinitiative.com.
21. Schumacher H, Kaiser E, Schnabel PA, Sykora J, Eckstein HH, Allenberg JR. Immunophenotypic characterisation of carotid plaque: increased amount of inflammatory cells as an independent predictor for ischaemic symptoms. Eur J Vasc Endovasc Surg. 2001; 21:494–501. [PubMed: 11397022]
22. Jander S, Sitzer M, Schumann R, et al. Inflammation in high-grade carotid stenosis: a possible role for macrophages and T cells in plaque destabilization. Stroke. 1998; 29:1625–1630. [PubMed: 9707204]
23. Carr SC, Farb A, Pearce WH, Virmani R, Yao JS. Activated inflammatory cells are associated with plaque rupture in carotid artery stenosis. Surgery. 1997; 122:757–763. [PubMed: 9347853]
24. van Leuven SI, van Wijk DF, Volger OL, et al. Mycophenolate mofetil attenuates plaque inflammation in patients with symptomatic carotid artery stenosis. Atherosclerosis. 2010; 211:231–236. [PubMed: 20202636]
25. van Wijk DF, Stroes ES, Dallinga-Thie GM. Novel insights into anti-inflammatory actions of HDL. Atherosclerosis. 2010; 212:388–389. [PubMed: 20650459]
26. Stein EA, Stroes ES, Steiner G, et al. Safety and tolerability of dalcetrapib. Am J Cardiol. 2009; 104:82–91. [PubMed: 19576325]
27. Duivenvoorden R, de Groot E, Stroes ES, Kastelein JJ. Surrogate markers in clinical trials—challenges and opportunities. Atherosclerosis. 2009; 206:8–16. [PubMed: 19327774]
28. Rudd JH, Narula J, Strauss HW, et al. Imaging atherosclerotic plaque inflammation by fluorodeoxyglucose with positron emission tomography: ready for prime time? J Am Coll Cardiol. 2010; 55:2527–2535. [PubMed: 20513592]
29. Alberti KG, Zimmet P, Shaw J. IDF Epidemiology Task Force Consensus Group. The metabolic syndrome: a new worldwide definition. Lancet. 2005; 366:1059–1062. [PubMed: 16182882]
30. Gami AS, Witt BJ, Howard DE, et al. Metabolic syndrome and risk of incident cardiovascular events and death: a systematic review and meta-analysis of longitudinal studies. J Am Coll Cardiol. 2007; 49:403–414. [PubMed: 17258085]
31. Van Gaal LF, Mertens IL, De Block CE. Mechanisms linking obesity with cardiovascular disease. Nature. 2006; 444:875–880. [PubMed: 17167476]
32. Rocha VZ, Libby P. Obesity, inflammation, and atherosclerosis. Nat Rev Cardiol. 2009; 6:399–409. [PubMed: 19399028]
33. Hotamisligil GS, Shargill NS, Spiegelman BM. Adipose expression of tumor necrosis factor-alpha: direct role in obesity-linked insulin resistance. Science. 1993; 259:87–91. [PubMed: 7678183]
34. Kim TN, Kim S, Yang SJ, et al. Vascular inflammation in patients with impaired glucose tolerance and type 2 diabetes: analysis with 18F-fluorodeoxyglucose positron emission tomography. Circ Cardiovasc Imaging. 2010; 3:142–148. [PubMed: 20061516]
35. Ouchi N, Walsh K. Adiponectin as an anti-inflammatory factor. Clin Chim Acta. 2007; 380:24–30. [PubMed: 17343838]

36. Komatsu M, Ohfusa H, Aizawa T, Hashizume K. Adiponectin inversely correlates with high sensitive c-reactive protein and triglycerides, but not with insulin sensitivity, in apparently healthy Japanese men. Endocr J. 2007; 54:553–558. [PubMed: 17575367]

37. Yoo HJ, Kim SE, Park MS, et al. Serum adipocyte fatty acid-binding protein is associated independently with vascular inflammation: analysis with 18F-fluorodeoxyglucose positron emission tomography. J Clin Endocrinol Metab. 2011; 96:E488–E492. [PubMed: 21159847]

38. Howard BV, Ruotolo G, Robbins DC. Obesity and dyslipidemia. Endocrinol Metab Clin N Am. 2003; 32:855–867.

39. Paulmier B, Duet M, Khayat R, et al. Arterial wall uptake of fluorodeoxyglucose on PET imaging in stable cancer disease patients indicates higher risk for cardiovascular events. J Nucl Cardiol. 2008; 15:209–217. [PubMed: 18371592]

40. Rominger A, Saam T, Wolpers S, et al. 18F-FDG PET/CT identifies patients at risk for future vascular events in an otherwise asymptomatic cohort with neoplastic disease. J Nucl Med. 2009; 50:1611–1620. [PubMed: 19759117]

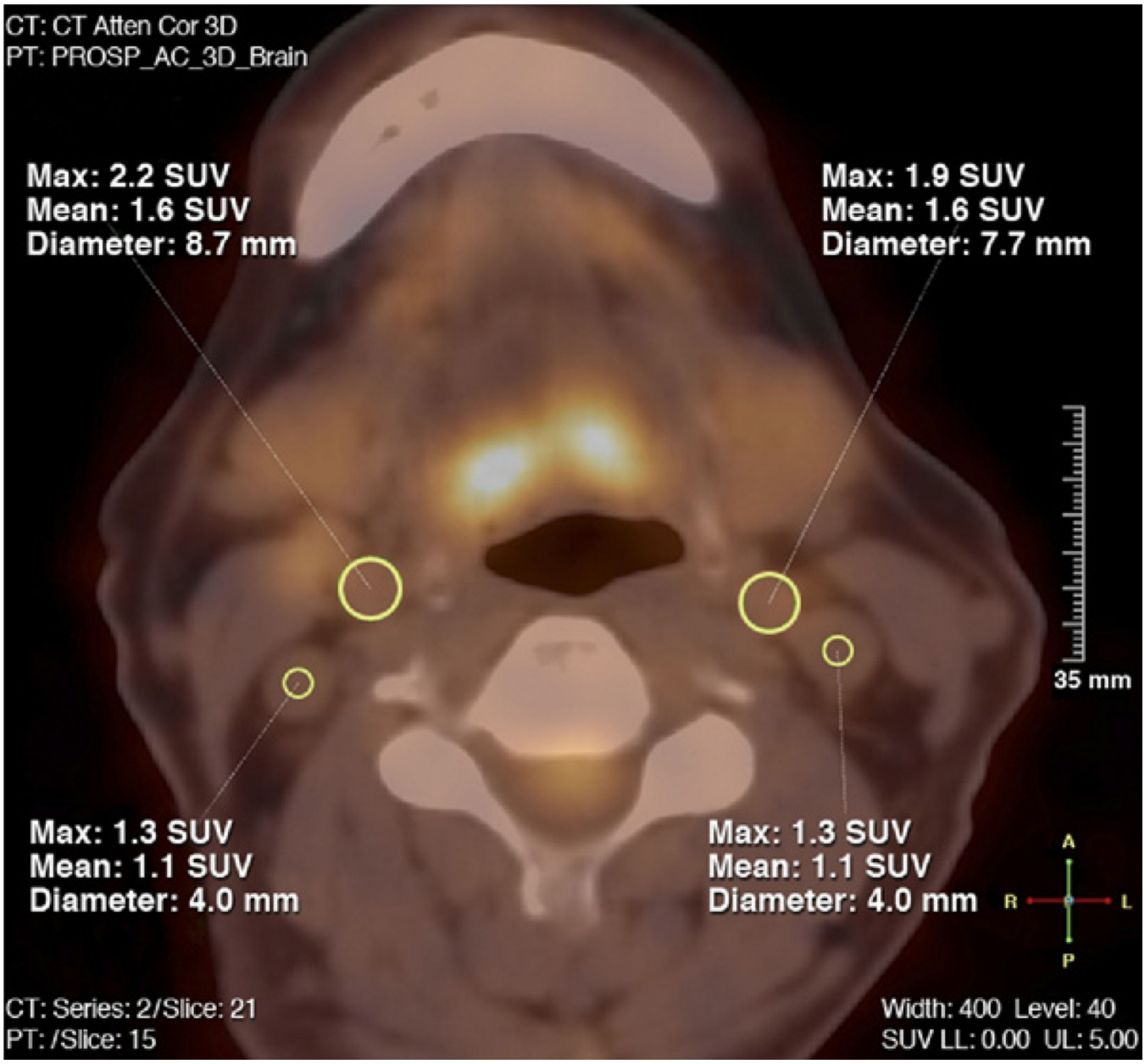

Figure 1. FDG-PET Image Analysis

This figure shows 1 slice of the fused positron emission tomography/computed tomography (PET/CT) images of the neck in transaxial view. Regions of interest (ROIs) (yellow) drawn around the outer border of the vessel walls of the left and right common carotid arteries, as well as, for evaluation of the 18F-fluorodeoxyglucose (FDG) blood pool activity, within the lumen of both jugular veins (SUV_{max}, SUV_{mean}, and diameter of the ROIs). SUV = standardized uptake value.

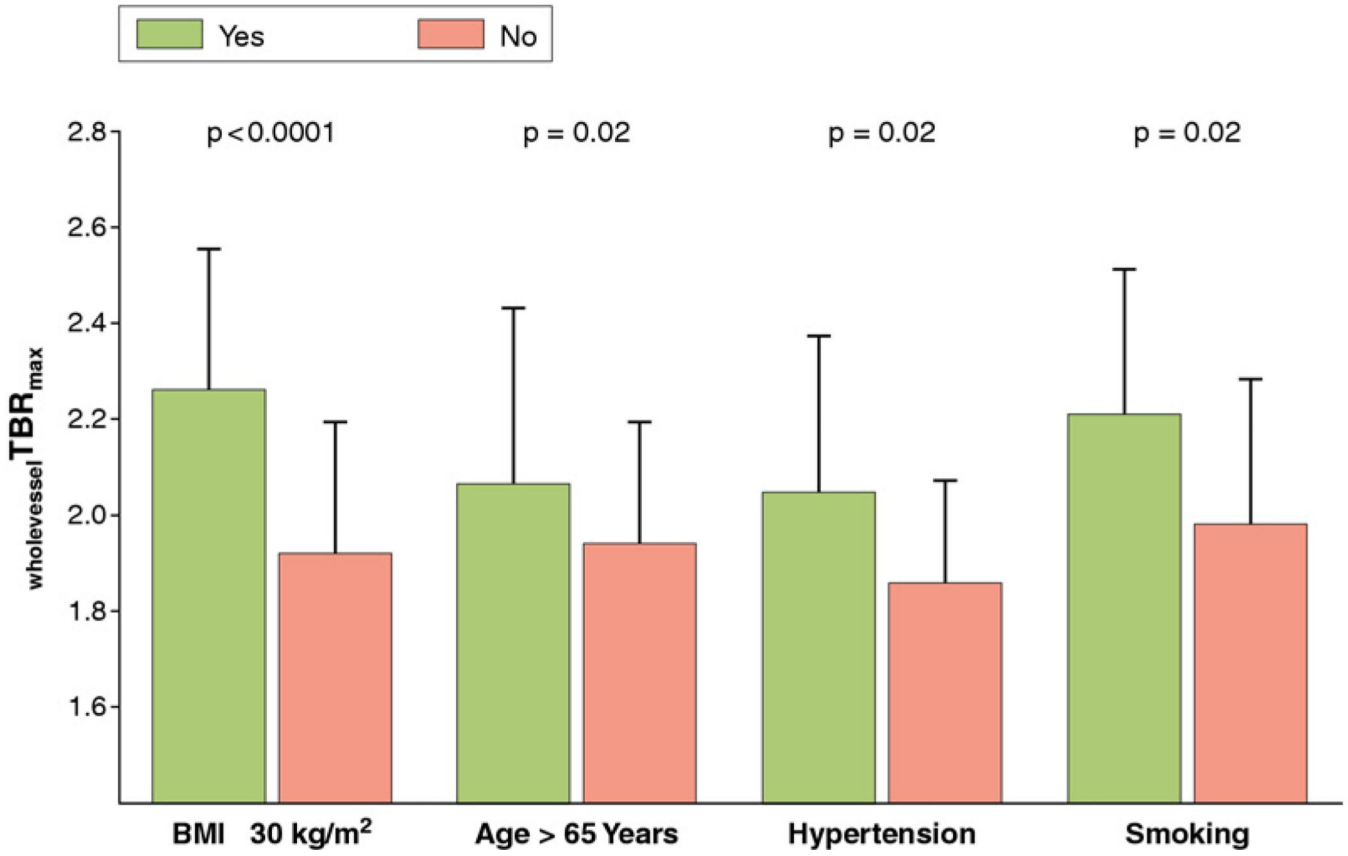

Figure 2. Clinical Risk Factors of Carotid Vessel Wall Inflammation in CAD Patients

This figure shows that body mass index (BMI) ≥30 kg/m^{2}age > 65 years, hypertension, and smoking are independent predictors for carotid wall inflammation as depicted by the whole-vessel target-to-background ratio ($_{wholevessel}TBR_{max}$). Bars represent standard deviations. p Values are adjusted for the other 4 predictors given in Table 2. CAD = coronary artery disease.

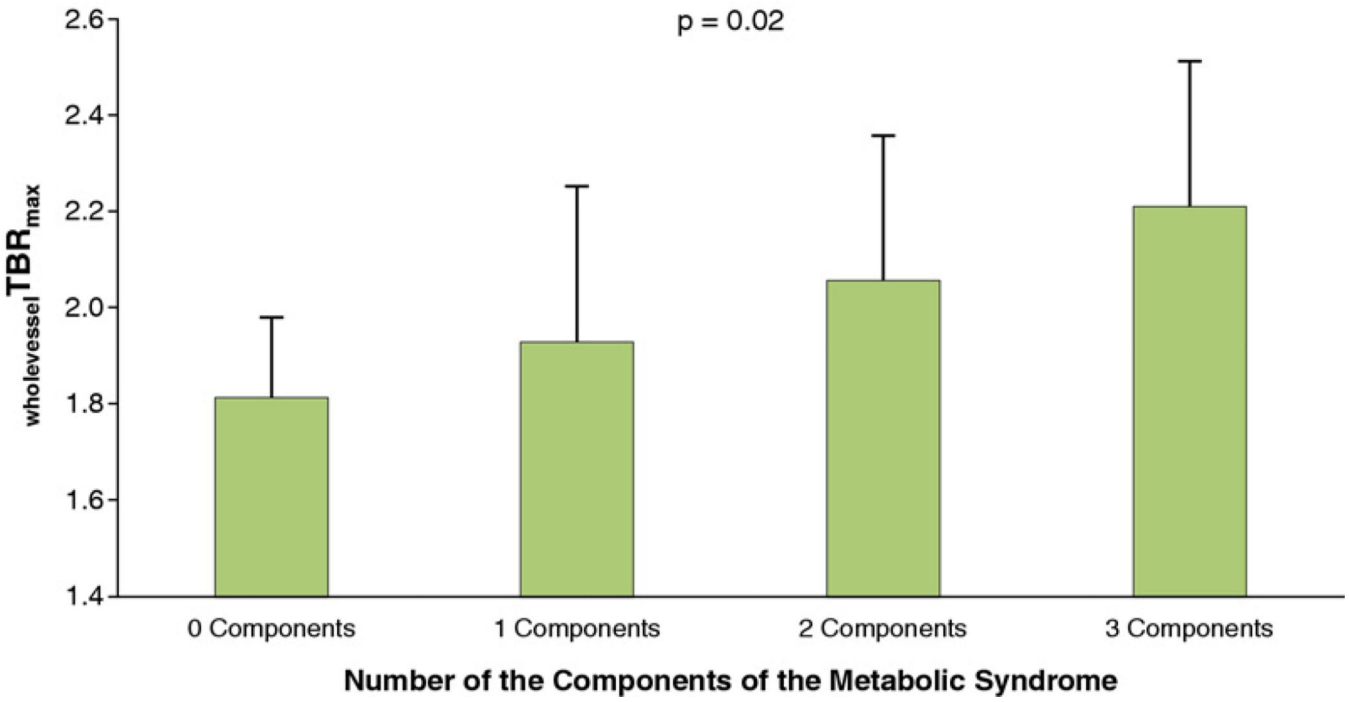

Figure 3. Relation Between the Metabolic Syndrome and Carotid Vessel Wall Inflammation

Whole-vessel TBR_{max} is whole-vessel maximum target-to-background ratio. Bars represent standard deviations. A 1-way analysis of variance was performed to test for between-group differences ($p = 0.02$).

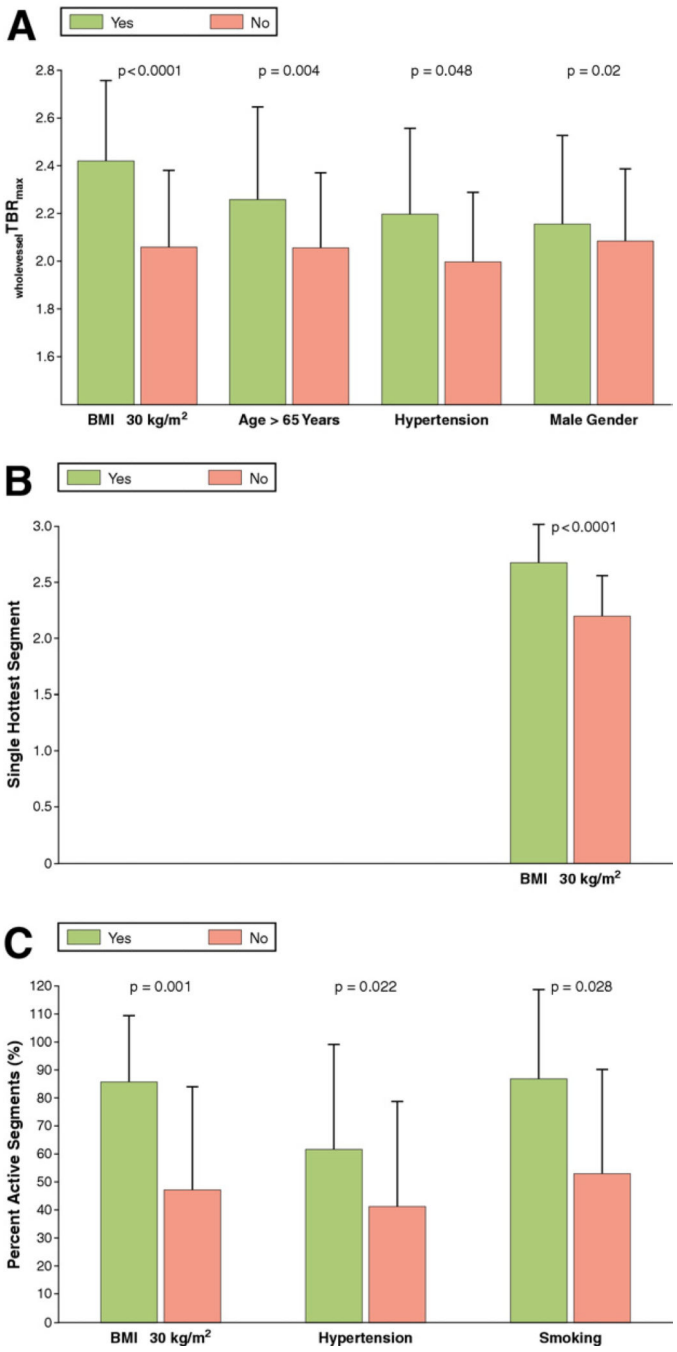

Figure 4. Clinical Risk Factors of Carotid Vessel Wall Inflammation in CAD Patients

This figure shows which CAD risk factors are independent predictors of carotid wall inflammation as depicted by $_{\text{wholevessel}}SUV_{\text{max}}$ (A), single hottest segment (B), and percent active segment (C). Percent active segments is defined as the percentage of segments with $TBR_{\text{max}} > 1.9$. Bars represent standard deviations. p Values for $_{\text{wholevessel}}SUV_{\text{max}}$ and for the single hottest segment are adjusted for the other 3 predictors given in Table 2; the p

value for the percent active segment is adjusted for the other 2 predictors. Abbreviations as in Figures 1 and 2.

Table 1

Characteristics of the CAD Population

Characteristics	n = 82
Age, yrs	62.0 ± 9.7
> 65	33 (40.2)
Gender	
Male	67 (81.7)
Female	15 (18.3)
BMI, kg/m^2	27.8 ± 4.1
BMI < 25	21 (25.6)
BMI ≥25 to < 30	40 (48.8)
BMI ≥30	21 (25.6)
Lifestyle	
Smoking	
Never	37 (45.1)
Former	38 (46.3)
Current	7 (8.6)
Alcohol users	32 (39.0)
Exercisers	50 (61.0)
Medical history	
Cardiovascular disease	
Myocardial infarction	32 (39.0)
Percutaneous transluminal coronary intervention	61 (74.4)
Coronary artery bypass surgery	23 (28.4)
Stroke/transient ischemic attack	3 (3.7)
Peripheral artery disease	4 (4.9)
Family history of cardiovascular disease	48 (58.5)
Hypertension	59 (72.0)
Duration of hypertension, months	133.9 ± 119.4
Diabetes	31 (37.8)
Type I diabetes	3 (3.7)
Type II diabetes	28 (34.1)
Duration of diabetes, yrs	12.5 ± 15.0
Fasting glucose, mmol/l	6.0 ± 1.5
Medication	
Statin	78 (95.1)
Duration, months	55.5 ± 73.5
Beta-blocker	50 (61.0)
Calcium-channel blockers	13 (15.9)
ACE inhibitors	32 (39.0)
AT II blockers	10 (12.2)
Nitrates	9 (11.0)

Characteristics	**n = 82**
Diuretics	13 (15.9)
Aspirin	75 (91.5)
Clopidrogrel	60 (73.2)
Insulin	6 (7.3)
Oral antidiabetics (metformin and/or others)	26 (31.7)
FDG-PET/CT	n = 79
Blood pool activity (left and right jugular vein; SUV_{mean})	1.08 ± 0.1
$_{wholevessel}TBR_{max}$	2.0 ± 0.3
$_{wholevessel}TBR_{max}$ > 1.8	55 (69.6)
$_{wholevessel}TBR_{max}$ > 2.0	32 (40.5)
$_{wholevessel}TBR_{max}$ > 2.2	19 (24.1)
$_{wholevessel}TBR_{max}$ > 2.4	10 (12.7)
$_{wholevessel}SUV_{max}$	2.14 ± 0.4
Single hottest segment	2.32 ± 0.4
Percent active segments	56.3 ± 37.7
0%	10 (12.7)
1%–30%	16 (20.2)
31%–60%	18 (22.8)
61%–90%	8 (10.2)
91%–100%	27 (34.2)

Values are mean ± SD or n (%). Percent active segments is defined as the percentage of segments with TBR_{max} > 1.9.

ACE = angiotensin-converting enzyme; AT II = angiotensin II; BMI = body mass index; CAD = coronary artery disease; FDG-PET/CT = 18F-fluorodeoxyglucose positron emission tomography/computed tomography; SUV_{max} = maximum standardized uptake value; TBR_{max} = maximum target-to-background ratio.

Table 2

Multiple Linear Regression Analyses With Backward Elimination to Identify Clinical Risk Factors of Carotid Vessel Wall Inflammation

	B	95% Confidence Interval	p Value
wholevesselTBRmax			
BMI ≥30 kg/m^2	0.29	0.15 to 0.44	< 0.0001
Age > 65 yrs	0.16	0.04 to 0.28	0.01
Hypertension	0.18	0.04 to 0.33	0.01
Smoking	0.27	0.04 to 0.51	0.02
Male	0.14	−0.02 to 0.30	0.09
wholevesselSUVmax			
BMI ≥30 kg/m^2	0.38	0.22 to 0.55	< 0.0001
Age > 65 yrs	0.22	0.07 to 0.36	0.004
Male	0.23	0.04 to 0.41	0.02
Hypertension	0.16	0.008 to 0.32	0.04
Single hottest segment			
BMI ≥30 kg/m^2	0.4	0.21 to 0.59	< 0.0001
Age > 65 yrs	0.2	0.03 to 0.36	0.018
Smoking	0.32	0.012 to 0.62	0.042
Hypertension	0.18	0.000 to 0.36	0.05
Percent active segments			
BMI ≥30 kg/m^2	30.8	12.58 to 49.0	0.001
Hypertension	21.9	4.57 to 39.22	0.014
Smoking	32.9	3.75 to 62.13	0.028

Whole-vessel target-to-background ratio ($_{\text{wholevessel}}\text{TBR}_{\text{max}}$), whole-vessel maximum standardized uptake value ($_{\text{wholevessel}}\text{SUV}_{\text{max}}$), single hottest segment, and percent active segments were the response variables, and the coronary artery disease risk factors age > 65 years, male gender, body mass index (BMI) ≥30 kg/m^2, smoking, alcohol use, exercise, hypertension, diabetes, fasting glucose levels, and family history of cardiovascular disease were the explanatory variables. Variables were retained in the model when $p < 0.10$. The best model is shown. B is the regression coefficient. Percent active segments is defined as the percentage of segments with TBR_{max} >1.9.